PCCP

Dynamic Article Links

Cite this: *Phys. Chem. Chem. Phys.*, 2012, **14**, 10690–10704

www.rsc.org/pccp

PAPER

Accurate spin–orbit and spin–other-orbit contributions to the *g*-tensor for transition metal containing systems†

A. Van Yperen-De Deyne, E. Pauwels, V. Van Speybroeck and M. Waroquier*

Received 4th April 2012, Accepted 22nd May 2012
DOI: 10.1039/c2cp41086a

In this paper an overview is presented of several approximations within Density Functional Theory (DFT) to calculate *g*-tensors in transition metal containing systems and a new accurate description of the spin–other-orbit contribution for high spin systems is suggested. Various implementations in a broad variety of software packages (ORCA, ADF, Gaussian, CP2K, GIPAW and BAND) are critically assessed on various aspects including (i) non-relativistic *versus* relativistic Hamiltonians, (ii) spin–orbit coupling contributions and (iii) the gauge. Particular attention is given to the level of accuracy that can be achieved for codes that allow *g*-tensor calculations under periodic boundary conditions, as these are ideally suited to efficiently describe extended condensed-phase systems containing transition metals. In periodic codes like CP2K and GIPAW, the *g*-tensor calculation schemes currently suffer from an incorrect treatment of the exchange spin–orbit interaction and a deficient description of the spin–other-orbit term. In this paper a protocol is proposed, making the predictions of the exchange part to the *g*-tensor shift more plausible. Focus is also put on the influence of the spin–other-orbit interaction which becomes of higher importance for high-spin systems. In a revisited derivation of the various terms arising from the two-electron spin–orbit and spin–other-orbit interaction (SOO), new insight has been obtained revealing amongst other issues new terms for the SOO contribution. The periodic CP2K code has been adapted in view of this new development. One of the objectives of this study is indeed a serious enhancement of the performance of periodic codes in predicting *g*-tensors in transition metal containing systems at the same level of accuracy as the most advanced but time consuming spin–orbit mean-field approach. The methods are first applied on rhodium carbide but afterwards extended to a broad test set of molecules containing transition metals from the fourth, fifth and sixth row of the periodic table. The set contains doublets as well as high-spin molecules.

1 Introduction

Theoretical calculations of magnetic resonance properties can be very useful to assist the interpretation and assignment of electron paramagnetic resonance (EPR) spectra. Several approaches for these calculations have been developed[1–8] which are very successful but often limited to relatively small systems in gas-phase calculations. Much less attention has been given to calculations in extended condensed-phase molecular systems.

Paramagnetic defects in the solid state (such as crystals) are preferentially investigated in periodic codes, where the full environment of the defect is incorporated in the model space in a natural and efficient way. The implementation of the *g*-tensor in periodic codes is rather scarce,[6,8–10] but already demonstrated its usefulness and success in predicting EPR parameters in radiation induced radicals formed in amino acids and proteins.[11–13]

Fully employing the periodicity, one can simulate much larger molecular systems which do not suffer from unphysical borders which are present in cluster-*in-vacuo* simulations. For these extended systems Density Functional Theory (DFT) is the most appropriate method, since the computation time is much smaller compared to other correlated methods, such as post-Hartree–Fock methods.

These periodic programs could be of considerable interest, *e.g.* to investigate transition metal containing materials such as transition metal defects in ionic lattices, transition metal doped zeolites, metal–organic frameworks or even bio-inorganic systems. However, the implementations of the *g*-tensor in programs with periodic boundary conditions such as CPMD,[6] CP2K,[9] GIPAW and BAND have only been scarcely applied to transition metal containing systems.[14,15]

Several studies have calculated EPR properties of transition metal substituted zeolites.[16–18] This spectroscopic technique is very sensitive to the transition metal environment and can be

Center for Molecular Modeling, Ghent University, Technologiepark, 903, B-9052 Zwijnaarde, Belgium. E-mail: michel.waroquier@ugent.be
† Electronic supplementary information (ESI) available: See DOI: 10.1039/c2cp41086a

very successfully used to characterise transition metal centers. However all of the *ab-initio* studies on EPR properties for these systems have used a cluster-*in-vacuo* gas-phase approach to calculate the *g*-tensor. These intrinsically periodic systems require a geometry optimization in periodic codes as the full crystalline structure is taken into account by imposing periodic boundary conditions in the simulation cell.

In these applications it is convenient or even necessary to be able to compute also the *g*-tensor and hyperfine tensors in their true periodic environment. However, a thorough benchmark study on the various implementations for the *g*-tensor in codes with periodic boundaries on systems containing a broad variety of transition metals is prerequisite before the various codes can be reliably applied to more complex and larger applications. The state-of-the-art electronic structure program packages for the computation of spectroscopic EPR parameters and in particular *g*-tensors are ADF,[19–21] ORCA 2.8.0,[22] Gaussian09,[23] Dalton[24] and Mag-ReSpect[25] (see Table 1).

Suitable periodic codes are however rather limited. The pioneering work of Pickard and Mauri[8] resulted in the GIPAW code[26] which is a post-processing module for Quantum ESPRESSO.[27] It uses plane wave functions and a reconstruction scheme for the core electrons. The calculation of EPR parameters, such as the *g*-tensor, has become available recently in CP2K[28–30] but no benchmark calculations with respect to transition metal complexes were performed. This code differs from the GIPAW implementation since it combines plane waves and traditional Gaussian basis sets to perform all-electron calculations. A third periodic code is BAND[31] which differs from most periodic codes since it does not use a plane wave basis set but Slater type orbitals as used in ADF. An overview of available properties and relativistic calculations is presented in Table 1.

Despite all the efforts, predictions of *g*-tensor for transition metal complexes are still more challenging than for organic systems. In this paper we show that one possible cause is the lack of efficient two-electron spin–orbit calculations. Both the direct spin–orbit (SO(2e)) and the spin–other-orbit interaction are revised by reformulating the spin–orbit mean-field approach in second quantization. While the same result is found for spin-$\frac{1}{2}$ systems, a term which was neglected in past studies arises for high spin systems. It originates from the direct spin–other-orbit contribution and can be introduced even in an effective potential method, for which the results are explicitly calculated in this work. Besides this contribution, the exchange contribution of the spin–other-orbit term is discussed in both the spin–orbit mean-field and the effective potential method.

Table 1 Availability of EPR and relativistic modules in several *ab-initio* packages. MAG-ReSpect and Dalton were not used in this work but are given for reference. *A*-tensor: hyperfine tensor, ZFS: Zero-Field-Splitting, DKH: Douglas–Kroll–Hess

	A-tensor	*g*-tensor	ZFS	ZORA	DKH	Periodic
ORCA	✓	✓	✓	✓	✓	
G09	✓	✓			✓	
ADF	✓	✓		✓		
Dalton	✓	✓	✓		✓	
ReSpect	✓	✓	✓		✓	
CP2K	✓	✓			✓	✓
GIPAW	✓	✓				✓
BAND	✓	✓		✓		✓

Before discussing the new approaches concerning the spin–other-orbit contribution, a benchmark is performed using existing methods in both periodic and gas-phase computational schemes to calculate EPR properties for transition metal containing systems. It is complementary to several other studies[7,8,25,32–34] as emphasis is on the impact of the various relativistic and spin–orbit approximations which are implemented in the various codes, with specific focus on the periodic ones. Focus is made on the *g*-tensor calculation, since this property in particular is sensitive to relativistic effects.

As a first test system the transition metal containing rhodium carbide (RhC) is chosen. Experimental data for this molecule are available for the *g*-tensor as well as for the internuclear distance. For this reason the system can very accurately be modeled without extra assumptions with respect to geometry optimization. In addition, the absence of a molecular environment enables a clear assessment of the different methods, without interference of the molecular environment.

This system is typically used as a model system for rhodium in surface chemistry[35,36] and the conclusions made in this study can be used as a validation for extension to more complex molecular structures using Rh or other transition metals.

The EPR spectra for RhC were measured by Brom *et al.*[37] in the gas phase, identifying an orthogonal and parallel component for the *g*-tensor (g_{ortho} = 2.0541 and g_{para} = 2.0039). Configuration interaction methods[36,38] and DFT methods[35] were applied previously to this system. These studies conclude that the wavefunctions predicted in DFT methods are described in a suitable manner.[35]

Subsequently, this benchmark investigation is extended to a set of other diatomic molecules in both doublet and high spin states. We have chosen the same set of molecules as used by Patchkovskii and Ziegler.[33] To allow a one-to-one correspondence, also the internuclear distances, which have been determined computationally in gas phase DFT calculations by these authors, have been used in this work for the computation of the different *g*-tensor contributions.

All the experimental *g*-factors of the diatomic molecules were found by EPR experiments in inert gases.[33,39–59]

Particular attention will be given to the new protocol proposed to treat SO exchange contributions to the *g*-tensor in effective potential models in a more accurate way and to the additional terms in the spin–other-orbit (SOO) contribution for high-spin ($S > 1/2$) molecules.

The structure of the paper is as follows: first the influence of various theoretical approaches and implementations for the *g*-tensor in non-periodic codes are investigated. In particular, special attention is devoted to relativistic corrections (Section 3.1), spin–orbit contributions (Section 3.2) and effects of choosing a suitable gauge (Section 3.3). For the spin–orbit coupling special care is given to the two-electron contributions in density based methods, more specific to how to approximate methods for the exchange integrals and to the derivation of the spin–other-orbit interaction. It is important to assess the importance of each of these models on the results as not all variants are implemented in periodic codes and one can determine the level of accuracy to be expected from these implementations (Section 4.1). Subsequently all conclusions are validated to a broad set of doublet and high spin diatomic

molecules which were also subject of previous theoretical papers[33,60] (Section 4.2 and Section 4.3).

2 Computational details

In order to assess each method for the calculation of the g-tensor on an equal footing, no optimization with respect to the internuclear distance was performed. The experimental value of $R = 1.613$ Å for RhC was systematically used as well as the same functional (PBE[61]) for all calculations.

For the sets of doublet and high-spin molecules in Sections 4.2 and 4.3, the reported internuclear distances by Belanzoni[60] and Patchkovskii[33] were used.

Several basis sets of increasing size were used to validate the dependence on basis set completeness. Whenever possible (ORCA, Gaussian09, CP2K), the Ahlrichs type basis sets of double-ζ (VDZ) and triple-ζ (TZV) quality were chosen.[62,63] Additional polarization functions (2df, dp, ppp)[64] and diffuse functions (p)[65] were introduced.

In ADF, Slater type basis sets of similar quality were used: a double-ζ (DZ) basis set without polarization functions and a triple-ζ basis set with one (TZP) polarization function. Both are frozen core basis sets up to the 3d and 4p shell.

Since the treatment of core electrons is of great importance for EPR parameters, the Gaussian Augmented Plane Wave (GAPW) method was chosen in the CP2K code.[66] This method does not solely use pseudopotentials, as is usually the case in periodic codes, but treats the core electrons with Gaussian Type Orbitals (GTO's) and valence electrons with a plane wave basis set. In our calculations the Ahlrichs type basis sets were augmented with plane waves up to 300 Rydbergs.

In the QuantumESPRESSO calculations the core region is not explicitly described since Troullier–Martins pseudopotentials[67] were used with a cutoff of 150 Rydbergs. They were generated based on relativistic atomic calculations. The GIPAW post-processing code uses a projector augmented-wave (PAW) like method[68] in which a linear transformation operator T is used to map the valence pseudo-wave functions to the corresponding all-electron wave function. Hence this description treats the core electrons adequately and can be used for accurate calculations of EPR properties.

For the calculation on the gas phase systems in CP2K and GIPAW, convergence with respect to the box size was investigated (see Section 5) and interactions between periodic images of the atoms and charge distribution were switched off. For the latter, the Martyna–Tuckerman Poisson solver[69] was used.

3 Methodological aspects

The g-tensor is defined as a second order property

$$g_{ij} = \frac{2}{\alpha}\frac{\partial^2\langle\Psi|H|\Psi\rangle}{\partial B_i \partial S_j}\bigg|_{\boldsymbol{B}=\boldsymbol{S}=0} \quad (1)$$

in which i and j indicate the Cartesian coordinate indices, α is the fine structure constant, $\boldsymbol{B}$ is the magnetic field and $\boldsymbol{S}$ is the spin operator. Note that in atomic units the Bohr magneton μ_B equals $\frac{\alpha}{2} = \frac{1}{2c}$. All further expressions throughout the paper will be given in atomic units.

The ground state Ψ is an implicit function of the external magnetic field $\boldsymbol{B}$ and double-perturbation theory is applied to evaluate the second order derivative. Eqn (1) yields different contributions arising from different terms in the perturbed Hamiltonian:

$$g_{ij} = g_e\delta_{ij} + \Delta g_{ij}^{ZKE} + \Delta g_{ij}^{SO,para} + \Delta g_{ij}^{SO,dia} + \Delta g_{ij}^{SOO} \quad (2)$$

Terms of the relativistic two particle Hamiltonian which are bilinear in both the spin and magnetic field give rise to the free electron g-factor ($g_e = 2.002319304$), the Zeeman Kinetic Energy contribution (Δg_{ij}^{ZKE}) and diamagnetic spin–orbit contributions ($\Delta g_{ij}^{SO,dia}$). The paramagnetic spin–orbit ($\Delta g_{ij}^{SO,para}$) and spin–other-orbit (Δg_{ij}^{SOO}) contributions result from terms linear in the electronic spin. The diamagnetic contributions $\Delta g^{SO,dia}$ arise due to the lack of gauge invariance of the magnetic vector potential.

Expressions for all these contributions can be found in the literature, though the formulation can vary.[1,7,9,26,34,70,71] In the further subsections of the methodological part, we only mention those expressions which are relevant to the discussion held in the paper.

Most packages compared in this study use the one-component method first proposed by Schreckenbach and Ziegler[70] in which the spin–orbit coupling is implemented in a perturbative way. For states represented by the $^n\Sigma$ molecular term symbol, such as the ground state of RhC,[36] this method cannot reproduce correctly the parallel component $g_{para} = g_e + \Delta g_{para}$ of the g-tensor since the first order spin–orbit terms vanish. No higher order spin–orbit contributions are taken into account and only small contributions such as the Zeeman kinetic energy and gauge terms are non-vanishing.[1] For this reason, the focus in this paper is on the orthogonal component of the g-tensor, which is substantially influenced depending on the specific spin–orbit or relativistic treatment.

Van Lenthe[3] derived a so-called two-component formalism, in which the Dirac Hamiltonian is appropriately transformed and the spin–orbit coupling is computed during the self-consistent-field iterations. For this non-perturbative calculation of the spin–orbit the g_{para} component is relevant even for $^n\Sigma$ states.

3.1 Relativistic effects

Relativistic effects are not negligible for transition metal containing systems. The most convenient choice is to use the Breit–Pauli Hamiltonian but this perturbation series is not valid near the nucleus. Van Lenthe *et al.* proposed the regular expansion[72] in which unperturbed states are those of the bound electrons. In zeroth order approximation this leads to the ZORA Hamiltonian.[72] Originally it was implemented in the two-component method in ADF, but van Wüllen[73] introduced a model potential which resulted in a computationally less expensive expression, which can be used as a scalar-relativistic method, *e.g.* as implemented in ORCA. Another commonly used relativistic Hamiltonian is the Douglas–Kroll–Hess Hamiltonian.[74] We refer to Table 1 for an overview of various implementations in the different software packages.

In ADF both the (unmodified) ZORA and Breit–Pauli approximations are implemented. Table 2 compares the results

Table 2 Calculated g-tensors ($\Delta g = g - g_e$) in parts per thousand (ppt) for RhC, calculated in ADF using relativistic two-component calculations with various basis sets. For these calculations Gauge Including Atomic Orbitals (GIAO) were used (see Section 3.3)

	Breit–Pauli		ZORA	
Basis set	Δg_{ortho}	Δg_{para}	Δg_{ortho}	Δg_{para}
DZ. 3d	62.92	−0.71	51.00	−0.46
DZ. 4p	58.59	−0.47	—	—
TZP. 3d	51.44	−0.38	52.78	−0.31
TZP. 4p	49.48	−0.32	51.22	−0.29
Exp	51.78	1.58	51.78	1.58

of both methods for the RhC molecule. Both are two-component methods and use the van Lenthe method to calculate g-tensors.[3] This method is not comparable to any method within the other programs used in this work since the spin–orbit operators are not treated perturbatively.

The ZORA results are in general in good agreement with the experimental values. When using the Breit–Pauli Hamiltonian, a good agreement is found when the triple-ζ basis sets are used.

3.2 Spin–orbit coupling

Spin–orbit coupling is the leading correction term in the g-tensor computation. It is relativistic in origin and therefore becomes much more important for heavy elements.

The reduction of the full Dirac equation to two-component equations results in the Breit–Pauli spin–orbit Hamiltonians (H^{BP}), which can be categorised in

(i) the one-electron spin–orbit–nucleus term

$$\hat{H}_{SO(N)} = \sum_i \frac{g'\alpha^2}{4} \sum_A Z_A s_i \cdot \frac{(\boldsymbol{r}_i - \boldsymbol{R}_A) \times \boldsymbol{p}_i}{|\boldsymbol{r}_i - \boldsymbol{R}_A|^3} \tag{3}$$

(ii) the two-electron spin–orbit term

$$\hat{H}_{SO(2e)} = -\sum_i \sum_{j \neq i} \frac{g'\alpha^2}{4} s_i \cdot \frac{(\boldsymbol{r}_i - \boldsymbol{r}_j) \times \boldsymbol{p}_i}{|\boldsymbol{r}_i - \boldsymbol{r}_j|^3} \tag{4}$$

(iii) the spin–other-orbit term

$$\hat{H}_{SOO} = -\sum_i \sum_{j \neq i} \alpha^2 s_i \cdot \frac{(\boldsymbol{r}_j - \boldsymbol{r}_i) \times \boldsymbol{p}_j}{|\boldsymbol{r}_i - \boldsymbol{r}_j|^3} \tag{5}$$

In eqn (3) Z_A represents the nuclear charge and $g' = 2g_e - 2$. The latter will be set to 2 in the remainder of the paper.

The direct calculation of the two-electron Hamiltonian matrix elements requires the evaluation of four-center integrals which are computationally very demanding. Several approximations have therefore been suggested, mainly based on the replacement of the two-body interaction by an effective one-electron operator, although contributions arising from the antisymmetric (or exchange) term are therefore completely neglected, which poses serious problems in the evaluation of the spin–other-orbit term (SOO). A reduction to a single-particle operator is most efficiently accounted for by means of some mean-field approach. As emphasized by Neese[71] a more quantitative accuracy is reached by explicit inclusion of the antisymmetric term. The different approaches, as proposed in the literature, will be tested on their reliability for the g-tensor computation for different isolated paramagnetic molecules with spin varying from 1/2 to 3. In particular the high spin radicals will be the subject of thorough investigation as they pose additional problems due to the presence of multiple singly occupied molecular orbitals.

3.2.1 Spin–orbit mean-field (SOMF).

We apply a somewhat different method than proposed by Neese[71] for the derivation of the antisymmetric (direct Coulomb + exchange) two-electron spin–orbit interaction $\hat{H}_{SO(2e)}$ and spin–other-orbit term $\hat{H}_{SOO}$. It relies on second quantization formalism and leads to additional contributions for high-spin molecules. Intermediary key steps are explained in the Appendix.

Completely similar to mean-field approaches, like Hartree–Fock, we define a spin–orbit mean-field $\hat{I}^{SO}$, which takes into account the interaction with all occupied orbitals:

$$\begin{aligned} \langle h|\hat{I}^{SO}|p\rangle &= \sum_{\alpha \in occ} \langle h\alpha|\hat{V}_{12}^{SO}|p\alpha\rangle_{as} \\ &= -\frac{1}{2}\sum_{a \in occ} \langle ha|\hat{L}_{1z}|pa\rangle + \frac{3}{4}\sum_{a \in occ} (\langle ha|\hat{L}_{1z}|ap\rangle + \langle ah|\hat{L}_{1z}|pa\rangle) \end{aligned} \tag{6}$$

with $\hat{V}_{12}^{SO} = \hat{V}_{12}^{SO(2e)} + \hat{V}_{12}^{SOO}$; h stands for the singly occupied orbital in the case of a spin-$\frac{1}{2}$ system and p any virtual orbital. Essential in the evaluation of the mean-field is the antisymmetric nature of the two-body interaction matrix elements including exchange terms besides the direct Coulomb contribution. $\boldsymbol{L}_1$ stands for some pseudo orbital momentum.

$$\boldsymbol{L}_1 = \frac{\alpha^2}{r_{12}^3}(\boldsymbol{r}_{12} \times \boldsymbol{p}_1) \tag{7}$$

which coincides with $-2g^{soc}(1,2)$ used by Neese.[71]

The different steps leading to the final expression of eqn (6) are outlined in the appendix. Use is made of the exact relationship between the exchange of the SOO and the SO(2e)

$$\sum_{\alpha \in occ} \langle h\alpha|V_{12}^{SOO}|\alpha p\rangle = 2\sum_{\alpha \in occ} \langle h\alpha|V_{12}^{SO(2e)}|\alpha p\rangle \tag{8}$$

which remains valid for high-spin systems (see Appendix).

Application of eqn (6) is the so-called spin–orbit mean-field (SOMF) approach, as implemented in ORCA. A similar method is the Atomic Mean-Field Integrals (AMFI) approach, where only one-center integrals are computed to further reduce the computational cost. Even this rather crude approximation performs quite well.[5]

The expression for the spin–orbit mean-field is slightly modified for high-spin complexes. The hp-pair also interacts with the singly occupied orbitals b, leading to some additional contributions in the direct Coulomb term:

$$\begin{aligned} \langle h|I^{SO}|p\rangle = &-\frac{1}{2}\sum_{a \in occ} \langle ha|L_{1z}|pa\rangle - \frac{1}{4}\sum_{b \in occ} \langle hb|L_{1z}|pb\rangle \\ &+ \frac{3}{4}\sum_{c=a,b \in occ} (\langle hc|L_{1z}|cp\rangle + \langle ch|L_{1z}|pc\rangle) \end{aligned} \tag{9}$$

In contrast to the spin-$\frac{1}{2}$ systems there is a non-vanishing contribution from the SOO interaction to the direct

Coulomb term

$$-\frac{1}{2}\sum_{b\neq\in\mathrm{occ}}\langle hb|L_{1z}|pb\rangle \qquad (10)$$

This term is new and hence not taken into consideration in earlier theoretical works.[71,75] It gives a non-negligible contribution to Δg^{SOO} as discussed in the computational results.

3.2.2 Effective potential within the KS-scheme. Explicit use of a two-body operator in a Kohn–Sham (KS) scheme is in principle inconsistent with the DFT concept. The direct Coulomb term for the two-electron spin–orbit interaction can easily be implemented with DFT, but the exchange contribution cannot be simulated within a one-body scheme. It is not surprising that the method as suggested by G. Schreckenbach and Ziegler[70] where the SO(2e) exchange contribution is modeled as ∇v_{xc} gives rise to arbitrary and thus unreliable results. Similarly it is excluded that the exchange part of the spin–other-orbit contribution can be evaluated within the Kohn–Sham scheme even approximately by using functionals specifically constructed to find an accurate ground state energy.

The effective potential method is based on the fact that the gradient of a Coulombic potential has the same radial dependence (*i.e.* $\boldsymbol{r}/r^3$) as the spin–orbit coupling. This is true for the external potential $v_{\mathrm{ext}}=\sum_A\frac{-Z_A}{|\boldsymbol{r}-\boldsymbol{R}_A|}$ and for the Hartree term $v_{\mathrm{H}}=\int\frac{\rho(\boldsymbol{r})}{|\boldsymbol{r}-\boldsymbol{r}'|}\mathrm{d}\boldsymbol{r}'$

The direct part of the two-body interaction can therefore exactly be reduced to an effective one-body potential

$$\hat{H}^{(1)}_{\mathrm{SO,Coul}}=\sum_i\frac{\alpha^2}{2}\boldsymbol{s}_i\cdot(\nabla v_{\mathrm{H}}(\boldsymbol{r})\times\boldsymbol{p}). \qquad (11)$$

Its contribution to the first order-perturbation energy expression, needed for the calculation of the g-matrix (see Appendix) readily becomes

$$\langle\Psi^{(0)}|\hat{H}^{(1)}_{\mathrm{SO,Coul}}|\Psi^{(1)}\rangle=\frac{\alpha^2}{2}\langle m_{s,h}|\boldsymbol{s}|m_{s,p}\rangle\cdot\langle h|\nabla v_{\mathrm{H}}(\boldsymbol{r})\times\boldsymbol{p}|p\rangle \qquad (12)$$

$$=-\frac{1}{2}\sum_{a\in\mathrm{occ}}\langle ha|L_{1z}|pa\rangle \qquad (13)$$

after inserting the electron density $\rho(\boldsymbol{r}')=\sum_{c\in\mathrm{occ}}\psi^*_c(\boldsymbol{r}')\psi_c(\boldsymbol{r}')$ determined by the Kohn–Sham orbitals ψ_c. $|\Psi^{(1)}\rangle$ represents the first order excitation of the KS ground state $|\Psi^{(0)}\rangle$, where the singly occupied orbital h is replaced by p.

So, the direct Coulomb two-electron distribution of eqn (4) is exactly reproduced by the effective one-body operator (11). On the basis of this exact relationship, this concept has been extended by Schreckenbach and Ziegler[70] and others,[6] to the whole Kohn–Sham potential $v_{\mathrm{KS}}=v_{\mathrm{ext}}+v_{\mathrm{H}}+v_{xc}$. In this way some effective spin–orbit interaction of one-body nature can be introduced:

$$H^{(1)}_{\mathrm{SO,eff}}=\sum_i\frac{\alpha^2}{2}\boldsymbol{s}_i\times(\nabla v_{\mathrm{KS}}(\boldsymbol{r})\times\boldsymbol{p}_i) \qquad (14)$$

This effective operator includes the gradient of the exchange correlation functional v_{xc} and one expected that it could mimic the exchange contribution of the two-electron spin–orbit interaction. Unfortunately, as it was already clearly reported by Neese,[71] numerical calculations undoubtedly demonstrate that the corrections arising from the ∇v_{xc} term are more or less of the same magnitude but with opposite sign compared to the exact exchange as calculated in the SOMF. We will come back extensively to this issue later on in the discussion section. Thus far about the two-electron spin–orbit interaction.

Regarding the spin–other-orbit coupling terms, within DFT there is no ready-made solution. Several approximations were suggested:

(i) It can completely be omitted (referred to V_{eff} method), as originally proposed by Schreckenbach and Ziegler.[70] These authors argued that this contribution is very small even if there is more than one unpaired electron. As correctly noticed by Neese[71] this is true for the direct Coulomb contribution in spin-$\frac{1}{2}$ molecules, but certainly not for the exchange term (see eqn (8)).

(ii) Another alternative is the method proposed by Pickard and Mauri[8] for the evaluation of the SOO correction. It is based on the screening of the external field B by the induced electronic currents, as experienced by the unpaired electron ($V_{\mathrm{eff,PM}}$).

$$\Delta g^{\mathrm{SOO}}_{xy}=\frac{1}{S}\int B^{1,x}_y(\boldsymbol{r})[\rho_\alpha-\rho_\beta]\mathrm{d}\boldsymbol{r} \qquad (15)$$

in which $B^{1,x}$ is the magnetic field induced by the electronic currents when a magnetic field with unit magnitude is applied in the x direction (referred to as $V_{\mathrm{eff,PM}}$).

(iii) The SOO exchange can be taken into account following its relation with the exchange of SO(2e) as established in eqn (8). This would imply that in the effective potential method the $\hat{H}^{(1)}_{\mathrm{SO},v_{xc}}$ contribution should be multiplied by a factor +3 to take into account the spin–other-orbit correction:

$$\Delta g(\mathrm{SO(2e)_{exch}})+\Delta g(\mathrm{SOO_{exch}})=\sigma\Delta g(\nabla v_{xc}) \qquad (16)$$

with $\sigma=3$.

However, as already noticed, the $H^{(1)}_{\mathrm{SO},v_{xc}}$ corrections have the wrong sign but roughly the same magnitude (factor 1.3 larger) as the exchange contribution of $V^{\mathrm{SO(2e)}}_{12}$. The scale factor σ switches to a value which can vary between −2 and −2.4. This procedure for computing the SOO exchange following the lines as expressed in eqn (16) with introduction of a scale factor σ is referred to as $V_{\mathrm{eff,SOO}(\sigma)}$. Neese[71] suggested a scale factor $\sigma=-2$ to achieve numerically the best agreement with the SOMF.[71] One of the goals of this work is to investigate the possible transferability of this scale factor to other paramagnetic systems and its dependence on the choice of the exchange correlation functional. Such an investigation has its large merits as it can be further explored to compute spin–orbit corrections to the g-tensor at the same accuracy as the SOMF method, but at a significantly less computational cost, especially for periodic purely density based codes.

(iv) Next to the scaling method, we found for high spin states an extra contribution for the direct SOO part as given by eqn (10). This term can also be written in the form

$$\langle\Psi^{(0)}|\hat{H}_{\mathrm{SOO,eff}}|\Psi^{(1)}\rangle|_{\mathrm{direct}}=\frac{\alpha^2}{2}\langle h|[\nabla v_{\mathrm{H}}[\rho_\uparrow-\rho_\downarrow](r)\times\boldsymbol{p}]_z|p\rangle \qquad (17)$$

Table 3 Overview of the various spin–orbit contributions to the $\Delta g_{\mathrm{ortho}}$ shift involved in the different methods. Exchange spin–other-orbit contributions are always evaluated according to the relation $\Delta g(\mathrm{SOO,exchange}) = 2\Delta g(\mathrm{SO(2e),exchange})$. In the effective potential method the exchange contribution of the two-electron spin–orbit interaction is evaluated through $\hat{H}^{(1)}_{\mathrm{SO},v_{xc}}$, multiplied with a scale factor σ as given in eqn (16). In this convention: $V_{\mathrm{eff}} = V_{\mathrm{eff,SOO}(\sigma=1)}$

			$\mathrm{SO(2e)_{exchange}}$		$\mathrm{SOO_{exchange}}$			
	SO(N)	$\mathrm{SO(2e)_{direct}}$	Two-body	∇V_{xc}	Two-body	∇V_{xc}	PM	$\mathrm{SOO_{direct}}$
Z_{eff}	✓							
V_{eff}	✓	✓		$\sigma = 1$				
$V_{\mathrm{eff,PM}}$	✓	✓		$\sigma = 1$			✓	
$V_{\mathrm{eff,SOO}}$	✓	✓		σ		✓		
$V^{*}_{\mathrm{eff,SOO}}$	✓	✓		σ		✓		✓
SOMF	✓	✓	✓		✓			

with $v_{\mathrm{H}}[\rho_{\uparrow} - \rho_{\downarrow}] = \int \frac{\rho_{\uparrow}(\boldsymbol{r}') - \rho_{\downarrow}(\boldsymbol{r}')}{|\boldsymbol{r} - \boldsymbol{r}'|} \mathrm{d}\boldsymbol{r}'$, which makes the implementation into CP2K much easier. In Section 4.3 we discuss the results of this new approach. This method, combined with the scaling of the exchange contribution, is referred to as $V^{*}_{\mathrm{eff,SOO}}(\sigma)$.

3.2.3 Effective nuclear charge (Z_{eff}). For completeness we also include a more simple approach which considers the two-electron spin–orbit Hamiltonian terms as screening terms for the one-electron H_{SON} contribution. One could neglect those two-electron contributions and compensate for them using an effective nuclear charge $Z_{A,\mathrm{eff}}$.[7,76–78] Eqn (3) is then rewritten as:

$$\hat{H}_{\mathrm{SO(N)}} = \sum_i \frac{g'}{4c^2} \sum_A Z_{A,\mathrm{eff}} \boldsymbol{s}_i \cdot \frac{(\boldsymbol{r}_i - \boldsymbol{R}_A) \times \boldsymbol{p}_i}{|\boldsymbol{r}_i - \boldsymbol{R}_A|^3} \qquad (18)$$

This simple approximation is available in several packages including Gaussian and ORCA.

For convenience of the reader an overview of the various models discussed in the paper is given in Table 3, including the various ingredients of the method. In Table 4 these are linked to the appropriate *ab initio* programs, including the new implementations.

3.3 Gauge

The vector potential $\boldsymbol{A}$ is defined up to an arbitrary translation. In principle the choice of this gauge should not influence any result, but basis set incompleteness causes a gauge dependency.

When using a common gauge origin (*e.g.* in ORCA) it is of interest to vary its position along the internuclear axis of the RhC molecule. This results in a maximum difference between the calculated g-values of $|g_{\mathrm{ortho}}(-1.2\ \text{Å}) - g_{\mathrm{ortho}}(1.2\ \text{Å})| \leq$ 1ppt which is much smaller than the effect of a relativistic Hamiltonian or the inclusion of the spin–other-orbit term (see below).

Table 4 *Ab-initio* packages–available spin–orbit approximations

	Z_{eff}	V_{eff}	$V_{\mathrm{eff,SOO}}$	$V^{*}_{\mathrm{eff,SOO}}$	$V_{\mathrm{eff,PM}}$	AMFI	SOMF
ORCA	✓	✓	✓				✓
G09	✓						
ADF		✓					
DALTON	✓					✓	
ReSpect	✓					✓	
CP2K		✓	✓	✓	✓		
GIPAW					✓		
BAND		✓					

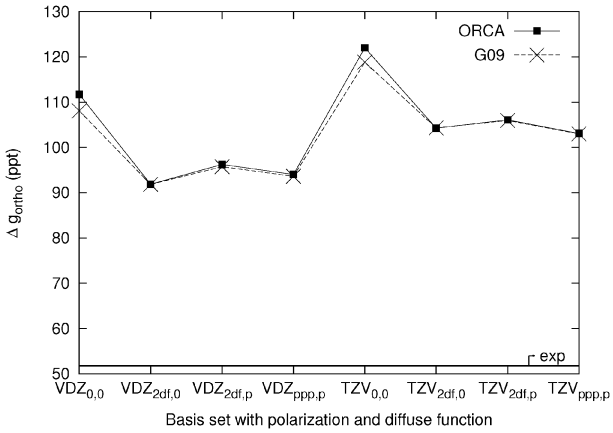

Fig. 1 Non-relativistic Gaussian09 results compared to the ORCA results. In both cases the Z_{eff} spin–orbit approximation was used. Both double (VDZ) and triple (TZV) ξ basis sets are used, to which several types of polarization (2df, ppp) and diffuse functions (p) are added, as indicated on the x-axis.

Another method which is commonly used is to include the gauge dependency into the atomic orbitals (Gauge Including Atomic Orbitals, GIAO[79]) as implemented in the Gaussian program and ADF (see Table 2). In Fig. 1 the Gaussian09 results using the Z_{eff} method (which is the only available option in Gaussian09) are compared with those of ORCA, in which a common gauge at the center of electronic charge was used. We can clearly see the agreement between both approaches. Additionally this figure shows that the gauge dependence is indeed due to a basis set incompleteness, as the differences are smaller for more extended basis sets.

The large discrepancies between experiment ($\Delta g_{\mathrm{ortho}} =$ 51.78 ppt) and computed results are caused by the use of a non-relativistic Hamiltonian and the Z_{eff} method, as will become clear further on.

4 Results and discussion

The focus of the paper is twofold. First we present a complete assessment study for the computation of the g-tensor for a spin 1/2 system containing a transition metal. We choose RhC as test case and discuss the predictions of the various models for the spin–orbit coupling as outlined in the methodology section.

Almost all spin–orbit models are implemented in ORCA. In addition, both relativistic and non-relativistic wave functions can be used, and a large choice of basis sets with polarization and diffuse functions is available in which the wave function can be expanded. For obvious reasons we choose ORCA as the reference non-periodic code for computation of *g*-tensors in gas-phase molecules.

Subsequently the ability of periodic codes to calculate accurately the *g*-tensor of RhC will be investigated. Although periodic codes are not ideally suited to model small isolated molecules, it is useful in this assessment study as the contributions of the different approaches for the *g*-tensor evaluation can easily be compared to their gas phase counterparts. The detailed comparison between the gas phase calculations and the various periodic results can give valuable information on how far the current protocols embedded in periodic codes are suitable to predict accurate *g*-tensors for more extended transition metal containing molecular systems for which standard gas phase calculations cannot be used due to the restrictions imposed on the cluster size.

Next to the preliminary conclusions drawn on the RhC compound, the other objectives of this study can only be accomplished if we extend the validation set to a wider range of molecules. We selected two sets of diatomic radicals used in previous benchmarks.[33,34,60] The first set consists of molecules with one unpaired electron,[34,60] while in the second set only high-spin radicals are taken up.[33] Both sets contain transition metal complexes and thus are relevant for the goal of this paper.

The second focus lies on the prediction of accurate spin–orbit contributions and in particular the exchange part of the two-electron spin–orbit term and the contribution of the spin–other-orbit interaction. In particular for paramagnetic high-spin molecules this discussion has not yet been held in the literature. Focus will also lie on the ability of periodic codes in predicting Δg shifts in close agreement with the spin–orbit mean-field method. The method proposed by Neese to overcome the anomaly present in the effective potential method for the prediction of the exchange contribution has been tested for a whole range of radicals and high-spin molecules.

For all molecules no further optimization has been performed: all geometrical parameters and the spin multiplicity of the energetically most favored configuration (for the high spin radicals) have been taken as reported in the literature.[33,60] When available the experimental values for the internuclear distances were taken for the spin-1/2 molecules. For more details concerning these sets we refer to the ESI.†

Discrepancies between the calculated *g* values and experimental EPR data for this test set can have several reasons: they can be due to the neglect of the molecular environment of the radical in the calculation (typically an inert matrix in the experiment), the internuclear distance might be incorrect (whether calculated or taken from X-ray diffraction experiments), or they indicate an inherent methodological failure of the approach used to calculate the *g*-tensor. In this work we will only concentrate on the last aspect.

To bias the influence of both experimental (internuclear distance, environment) and computational (exchange-correlation functional) errors and focus on the computational accuracy of the method under investigation, we opted to choose computational reference values of high quality calculations.

4.1 RhC as a test case for spin-$\frac{1}{2}$ systems

Rhodium is an element of the second transition row ($Z = 45$) with electronic structure $[Kr]^4d^85s^1$. RhC has a $^2\Sigma^+$ ground state with the unpaired electron in a molecular orbital constructed by the $4d_z^2$ and 5s orbitals of rhodium and the orbital $2p_z$ character of carbon.

The *g*-tensor anisotropy is large: 51.78 ppt for the orthogonal and 1.58 ppt for the parallel component. The prediction for the parallel component of the *g*-tensor is independent of the choice of the spin–orbit approximation and the basis set. A constant value of 0.22 ± 0.01 ppt is found. This is in full agreement with the fact that the Schreckenbach and Ziegler method cannot calculate the g_{para} for molecules with $^n\Sigma$ molecular term symbols.[1] Table 5 collects the various model predictions for the orthogonal Δg_{ortho} contributions in RhC.

4.1.1 Effect of relativistic Kohn–Sham orbitals and basis set dependence. A first survey concerns the impact of a relativistic approach on the g_{ortho} tensor values. Table 5 reveals that relativistic effects give rise to a shift of the *g*-tensor predictions with respect to the non-relativistic results, independently of the spin–orbit coupling method taken into account. The non-relativistic

Table 5 Calculation of the orthogonal component of the *g*-tensor (Δg_{ortho} in ppt) in RhC using the PBE functional in ORCA. Different models and basis sets are considered: non-relativistic *versus* relativistic models and contributions from the various spin–orbit approaches are reported. In $V_{eff,SOO}$ a scale factor of −2 is considered. Relativistic model makes use of the ZORA approach and the common gauge at the center of electron charge. The parallel component g_{para} is not tabulated as the same value (0.22 ± 0.01ppt) is found in all cases

	ORCA								CP2K		
	Relativistic				Nonrelativistic				Nonrelativistic		
	Z_{eff}	V_{eff}	$V_{eff,SOO}$	SOMF	Z_{eff}	V_{eff}	$V_{eff,SOO}$	SOMF	V_{eff}	$V_{eff,PM}$	$V_{eff,SOO}$
VDZ	89.62	62.51	52.27	51.97	111.73	70.72	66.06	65.69	70.80	70.73	67.63
VDZ, 2df	80.02	55.80	46.32	46.05	91.89	57.61	53.66	53.34	58.01	58.00	55.30
VDZ, 2df, p	82.47	56.44	47.83	47.55	96.27	60.45	56.33	56.00	60.63	60.58	57.82
VDZ, ppp, p	81.07	55.33	47.05	46.78	94.03	59.06	55.04	54.71	59.30	59.26	56.56
TZV	98.69	56.26	58.14	57.80	122.04	77.81	72.69	72.27	78.17	78.13	74.52
TZV, 2df	88.56	49.94	51.82	51.50	104.28	66.04	61.59	61.21	66.64	66.61	63.42
TZV, 2df, p	89.56	51.54	52.42	52.10	106.09	67.22	62.68	62.30	67.61	67.59	64.35
TZV, ppp, p	87.81	50.69	51.39	51.08	103.08	65.29	60.88	60.52	65.76	65.75	62.58
Exp	51.78	51.78	51.78	51.78	51.78	51.78	51.78	51.78	51.78	51.78	51.78

predictions are overestimated and strongly affected by the choice of the basis set. Indeed, inclusion of polarization functions leads to significant decrease of the orthogonal component of the g-tensor. The relativistic ZORA-predictions, however, reproduce the experimental value systematically better. The dependence on the presence of polarization functions is less dramatic. When the most advanced spin–orbit approximation, SOMF, is used, both double- and triple-ζ basis sets yield a more pronounced convergence behavior towards experiment with preference to the triple-ζ, which converges towards the experimental g_{ortho}. With a double-ζ basis set, without polarization or diffuse functions, the experimental g_{ortho} is even correctly reproduced, which is most likely a coincidence, but which should be verified in other transition metal doublets.

4.1.2 Spin–orbit approximation. From Table 5, it is clear that the most rudimentary approach (Z_{eff}) performs poorly as it systematically overestimates the experimental data by more than 28 ppt in the relativistic case and even twice this value in the non-relativistic treatment. This method is not appropriate to investigate systems containing transition metals.

The effective potential approximation (V_{eff}) performs much better, despite the unphysical behavior of the $\Delta g(\nabla v_{xc})$ contribution. But as this correction term is small, it does not significantly affect the global Δg shift. Compared to the Z_{eff} results, this approach almost always causes a rise of $\Delta g_{\mathrm{ortho}}$ by about 40 ppt, yielding a much better agreement with experiment.

The agreement further improves if we correct the wrong sign of the effective $\Delta g(\nabla v_{xc})$ contribution ($\sigma = -1$), but it becomes even much better if we consider a scale factor $\sigma = -2$ ($V_{\mathrm{eff,SOO}}$) following the suggestion of Neese, in this way incorporating the spin–other-orbit interaction in the effective potential method, as discussed in the theoretical section. The predictions of the Δg shift with SOMF don't differ much from $V_{\mathrm{eff,SOO}(\sigma=-2)}$, but this is due to the choice of the scale factor. We come back to this issue later in the discussion.

What conclusion can be drawn from Table 5 about the methodology reproducing as best the experimental g-tensor in the case of RhC? In both relativistic and non-relativistic approaches the best performing method is SOMF, followed by the $V_{\mathrm{eff,SOO}(\sigma=-2)}$ method. The former is much more expensive in computation time, while the latter is computationally favorable as no two-body matrix elements have to be evaluated, especially for periodic codes. The remarkable property that the effective exchange contribution scales linearly with SOMF makes this approach the most favorable for larger radicals. It fails when the linear relationship with the SOMF result does no longer hold or when the scale factor is strongly varying throughout the training set. Therefore the accuracy of the $V_{\mathrm{eff,SOO}(\sigma)}$ method will depend on this behavior and will be the subject of study in the remainder of this paper.

Concluding, the two SOMF and $V_{\mathrm{eff,SOO}(\sigma)}$ methods, both including spin–other-orbit interactions perform the best, and in view of the significantly larger computation time for the SOMF method, we could give preference to the $V_{\mathrm{eff,SOO}(\sigma)}$ method, but this should be confirmed by additional calculations on other systems.

4.1.3 Box size dependence on periodic codes. When applying a periodic code on an isolated molecule, the periodic cell should be large enough to prevent unphysical interactions originating from nearby periodic images or boundary conditions. Only under these conditions a reliable comparison with previous results can be made. The CP2K prediction for the orthogonal component of the g-tensor at different box sizes is plotted in Fig. 2. It shows a nice convergence behavior towards the ORCA result, using the same basis set (TZV), functional (PBE) and spin–orbit approximation (V_{eff}). For this small test system with a molecular size of about 1.613 Å, a box size of 12 Å is sufficient to yield an almost completely converged value.

A similar calculation is performed to test the box size dependence of the GIPAW predictions. It is expected that they approach the relativistic ORCA results with ZORA and the V_{eff} method. Due to the inherent usage of plane waves and pseudopotentials in GIPAW a direct comparison to a specific basis set choice in ORCA is not possible. Therefore we consider a range of width 6 ppt, determined by the ORCA–ZORA g_{ortho} values belonging to a TZV basis with various polarization and diffuse functions (see Fig. 2), as a reference for the convergence in GIPAW. Convergence is only reached at very large box sizes (at least 18 Å). This is an undesirable side effect, as large box sizes are computationally very demanding since a huge number of plane waves is required to describe the *vacuo*. This unfavorable aspect with respect to non-periodic codes has no serious consequences for truly periodic systems (*e.g.* defects in salts[15] or zeolites).

BAND on the other hand does not show a typical converging behavior as other periodic codes, but rather exhibits a fluctuating pattern when increasing the box size (Fig. 3). This is probably caused by interactions between periodic images which cannot be turned off in this program.

For the calculation of EPR properties, it is recommended to use an all electron approach. In GIPAW the core electrons are reconstructed, while BAND uses frozen core atoms for heavy elements. In CP2K the g-tensor can be determined from both

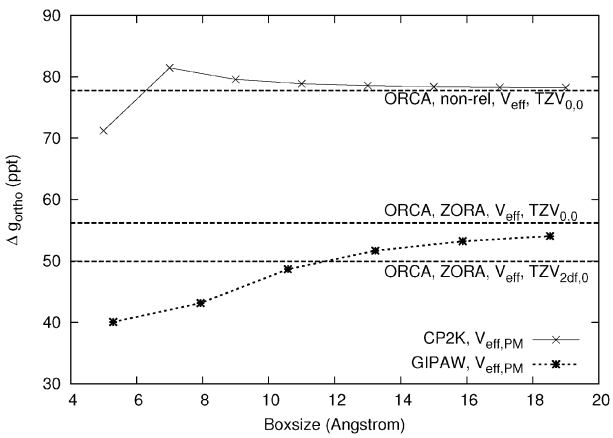

Fig. 2 Box size dependency of the orthogonal component of the g-tensor using the periodic CP2K (non-relativistic, TZV, V_{eff}) and GIPAW code (relativistically corrected pseudopotentials). Reference values are taken from ORCA (TZV basis, V_{eff}) and a range of values generated by ORCA (V_{eff}, ZORA) using a TZV basis set and several diffuse and polarization functions.

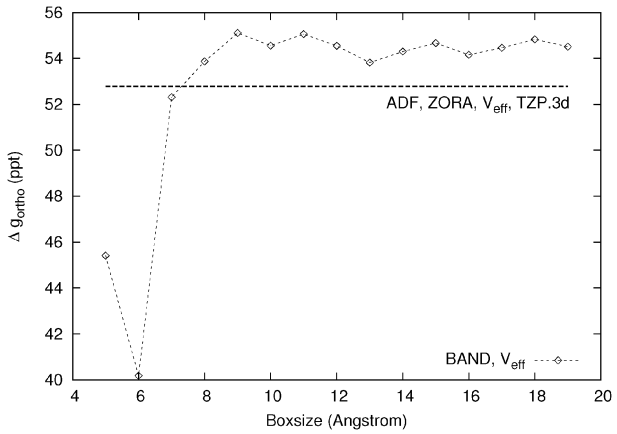

Fig. 3 Box size dependency of the orthogonal component of the *g*-tensor using BAND (TZP.3d basis set). The reference value is an ADF result with the same basis set.

pseudopotential (GPW) and all-electron (GAPW) wavefunction calculations. The GPW method fails to reproduce the experimental data. When 36 core electrons were considered, a Δg of -0.84 ppt was found. Use of a smaller set of core electrons (28) yields no improvement ($\Delta g = -2.22$ ppt). This could be caused by the inaccurate description of the valence electrons in this core region. Therefore, the computationally more expensive all electron GAPW method is highly recommended for *g*-tensor calculations on radicals.

In the current versions of CP2K and GIPAW the $V_{\mathrm{eff,PM}}$ method is the highest level present for the computation of the spin–orbit matrix elements, whereby the spin–other-orbit correction is computed using the Pickard and Mauri (PM) scheme (see theoretical section). From Table 5 it is clear that this spin–other-orbit term is negligible and even shows the wrong sign. As already mentioned the accuracy of the CP2K prediction can seriously be improved by implementing the $V_{\mathrm{eff,SOO}(\sigma)}$ method with $\sigma = -2$ or even a higher value for the scale factor (see further discussion) and inclusion of the direct SOO contribution for high spin systems. In Table 5 both V_{eff} and $V_{\mathrm{eff,SOO}}(\sigma)$ results obtained in ORCA and CP2K are given. They show a nice agreement despite the difference in the choice of gauge.

4.2 Radical doublets (spin 1/2 systems)

The next two subsections will be devoted to the reproduction and the discussion of the various spin–orbit contributions, which lie on the origin of the observed Δg shift from the free electron g_e value. Conclusions drawn for the specific RhC case will be further assessed to a wider range of molecules. The most advanced SOMF method can be taken as reference model, but the performance of the effective $V_{\mathrm{eff,SOO}(\sigma)}$ method will receive special attention due to the significantly less computational cost, the more as in periodic codes as CP2K *g*-tensor calculations are based on the DFT-based effective potential method. In particular the behavior of the scale factor σ will be assessed on its robustness.

First we select a set of diatomic radicals, which already has been used in earlier benchmark studies.[33,34,60] They are listed in Tables 6 and 7 and ordered according to the position of the heaviest element in the periodic table. Experimental Δg shifts are taken from the literature.[60] For all ORCA results a triple-ζ quality basis set with polarization functions (Ahlrichs 2df) was used.

In Table 6 the several contributions to the *g*-tensor are listed to give insight into the importance of each spin–orbit term. Both ORCA and CP2K results are present, however the SO(N) part is only calculated separately using ORCA. The Zeeman Kinetic Energy part (ZKE) is identical for both codes and therefore only reported for ORCA.

The one-electron contribution SO(N) is the trendsetter whether *g* will deviate largely from the free electron value. All species reporting a *g* value significantly different from the free-electron *g*-value report a large SO(N) contribution. In most of the cases the prediction of SO(N) overshoots the observed Δg shift. This is best illustrated with PdH exhibiting the largest deviation from g_e and whose experimental Δg tensor value amounts to 290.88 ppt. From all spin 1/2 molecules

Table 6 Various spin–orbit contributions to the $\Delta g_{\mathrm{ortho}}$ shift(in ppt) for several radical doublets. All calculations were performed with PBE and Ahlrichs TZV, 2df basis set. The scaling factors σ and σ' are defined in eqn(19) and (20) respectively

		ORCA					CP2K			
					SO(2e)$_{\mathrm{exch}}$					
	Exp	ZKE	SO(N)	SO(2e)$_{\mathrm{dir}}$	SOMF	∇v_{xc}	SO(N) + SO(2e)$_{\mathrm{dir}}$	(∇v_{xc})	σ	σ'
RhC	51.78	−0.144	83.680	−18.990	−1.110	1.485	65.869	1.311	−2.24	−2.54
BO	−1.72	−0.095	−2.832	0.790	0.129	−0.174	−1.750	−0.120	−2.22	−2.21
BS	−8.12	−0.107	−11.571	1.822	0.263	−0.362	−9.063	−0.259	−2.18	−3.05
AlO	−1.22	−0.181	−2.861	0.455	0.015	−0.016	−2.545	0.007	−2.85	6.68
GaO	−34.32	−0.234	−37.676	2.360	−0.028	0.006	−35.642	0.030	−14.59	−2.84
ScO	−0.52	−0.070	−1.263	0.912	0.074	−0.091	−0.203	−0.058	−2.45	−3.82
ZnH	−17.12	−0.096	−17.648	1.255	0.154	−0.233	−16.030	−0.162	−1.99	−2.85
ZnF	−6.32	−0.152	−7.309	0.426	0.056	−0.084	−6.878	−0.013	−2.03	−13.45
ZnAg	−11.82	−0.066	−20.200	2.535	0.208	−0.307	−17.124	−0.195	−2.03	−3.20
YO	−0.22	−0.071	−1.778	0.968	0.064	−0.082	−0.695	−0.050	−2.34	−3.80
PdH	290.88	−0.348	344.702	−79.558	−4.664	6.323	250.802	4.765	−2.21	−2.94
CdH	−49.92	−0.098	−55.316	3.102	0.326	−0.481	−51.340	−0.358	−2.03	−2.73
CdF	−17.32	−0.154	−21.812	1.385	0.129	−0.186	−20.211	−0.133	−2.08	−2.91
CdAg	−31.22	−0.072	−60.136	4.696	0.356	−0.579	−54.459	−0.379	−1.85	−2.82
InO	−192.32	−0.247	−110.208	5.635	0.254	−0.396	−104.067	−0.332	−1.93	−2.30

Table 7 Complete Δg_{ortho} in ppt for spin-$\frac{1}{2}$ systems

		ORCA			CP2K	
	Exp	SOMF	V_{eff}	$V_{eff,SOO}$ ($\sigma = -2$)	V_{eff}	$V_{eff,SOO}$ ($\sigma' = -2.8$)
RhC	51.78	72.29	77.79	72.69	67.04	61.79
BO	−1.72	−1.75	−2.31	−1.79	−2.29	−1.81
BS	−8.12	−9.07	−10.22	−9.13	−10.25	−9.21
AlO	−1.22	−2.54	−2.60	−2.56	−2.54	−2.56
GaO	−34.32	−35.63	−35.54	−35.56	−35.45	−35.57
ScO	−0.52	−0.20	−0.51	−0.24	−0.46	−0.23
ZnH	−17.12	−16.03	−16.72	−16.02	−16.82	−16.18
ZnF	−6.32	−6.87	−7.12	−6.87	−5.99	−5.94
ZnAg	−11.82	−17.11	−18.04	−17.12	−17.19	−16.41
YO	−0.22	−0.69	−0.96	−0.72	−0.80	−0.60
PdH	290.88	250.80	271.12	252.15	269.63	250.57
CdH	−49.92	−51.33	−52.79	−51.35	−53.27	−51.84
CdF	−17.32	−20.19	−20.77	−20.21	−20.27	−19.74
CdAg	−31.22	−54.44	−56.09	−54.35	−52.56	−51.04
InO	−192.32	−104.06	−105.22	−104.03	−105.50	−104.17

of the training set indeed PdH predicts the largest spin–orbit–nucleus correction, but with 344.70 ppt it overestimates the experimental value with 54 ppt.

The direct Coulomb correction cancels for a part the excess of the SO(N) contribution. It has systematically another sign, and is essential to go closer to the experimental value. We don't see some systematics in its magnitude with respect to the most dominant SO(N) value. Its relative importance with respect to the SO(N) value varies from 5% to more then 50%.

In only one case (InO) the one-electron contribution is largely insufficient for explaining the experimental behavior. With a contribution of −110 ppt it is by far too small to come in the vicinity of the experimental value of −192 ppt. Two-electron spin–orbit contributions are insufficient to compensate this underestimation of the one-electron part.

For the exchange contribution of the SO(2e) part, both the SOMF and the V_{eff} method were used and compared. It is clear from the table that there is a systematic difference of the predictions in both approaches. According to relation (16) discussed in previous section, we report in Table 6 the scale factor σ relating the exchange contribution of the SOMF two-electron term and the effective SO(2e; ∇v_{xc}) prediction. It is determined by

$$\sigma = -\frac{3\Delta g(\mathrm{SO(2e)_{exch,SOMF}})_{\mathrm{ORCA}}}{\Delta g(\nabla v_{xc})_{\mathrm{ORCA}}} \qquad (19)$$

and shows a remarkable tendency to −2 which almost coincides with the suggested value of Neese. This is a highly remarkable behavior and we can make use of it to switch the unrealistic DFT exchange correction SO(2e; ∇v_{xc}) to a reliable value which nicely reproduces the exact exchange obtained from a procedure that needs a much larger computational cost. At the same time the SOO contribution can be taken into account in view of the relation with the two-electron exchange term.

We also include the results obtained with the periodic code CP2K, making use of the effective potential method. Despite the same functional has been employed and the same exchange-correlation functional v_{xc} for the evaluation of the SO(2e; ∇v_{xc}) contribution, we notice some discrepancies in the values predicted by the non-periodic code ORCA. The SO(2e; ∇v_{xc}) contributions are systematically underestimated with respect to their ORCA counterparts. We propose the same procedure as in ORCA in introducing a scale factor σ' relating the CP2K exchange predictions to the exact SO(2e;exch) in SOMF.

$$\sigma' = -\frac{3\Delta g(\mathrm{SO(2e)_{exch,SOMF}})_{\mathrm{ORCA}}}{\Delta g(\nabla v_{xc})_{\mathrm{CP2K}}} \qquad (20)$$

This procedure offers a suitable protocol to overcome the obstacle of unphysical reproduction of exchange values under conditions that the new scale factor σ' also behaves almost constant throughout the training set. The last column in Table 6 indeed confirms that for the radical doublets the scale factor fluctuates between −2.30 and −3.80 with some minor exceptions. The agreement with the computationally more expensive SOMF-ORCA calculations is even largely improved if we apply a scale factor of about −2.80 through the whole set, but this scaling procedure remains some effective approach which requires confirmation in other training sets. The value of −2.80 is in magnitude somewhat larger than the scale factor proposed by Neese, but this is due to the systematic underestimation of the exchange contribution in the periodic CP2K code. There are some exceptions like AlO and ZnF where the scale factor σ' leaps out to +6.68 and −13.45. For these two cases the absolute values of the exchange contributions are particularly small, generating large error bars. Even when applying the effective value of −2.80 for σ' the global spin–orbit Δg shift in these molecules will be hardly affected.

The exchange part has the same sign but is smaller than the direct Coulomb contribution. To estimate its full impact, the numbers of the column $\mathrm{SO(2e)_{exchange}}$ (SOMF) in Table 6 should be multiplied with factor 3 in order to fully take into account the SOO effect. For spin 1/2 systems and in case the g-shift is larger than 5 ppt, the exchange can represent almost 2–8% of the total SO contribution. This is in line with the observations made by Neese. It is by far not the leading term. However, in cases where the deviation of the g-tensor from the free electron value is small, it can even dominate.

Adding up the different individual contributions in Table 6, we get the total Δg_{ortho} values for all diatomic spin-$\frac{1}{2}$ systems (Table 7). In Neese[71] work the different SO operators have been assessed to a training set of small organic molecules with spin 1/2. The $V_{eff,SOO}(\sigma = -2)$ came out as most accurate, and in fact our results on a completely different training set lead to the same findings.

The overall agreement with experiment is more than satisfactory (see Table 7). The total SOMF predictions succeed in reproducing the experimental fluctuations of the g-tensor from the free electron value taking place in the training set of radical doublets. The two molecules showing the largest deviation have already been discussed: InO and RhC. Use of relativistic wave functions can resolve this discrepancy in the case of RhC. For InO the use of relativistic methods improves the results as well (up to −124.7 ppt) but the relativistic correction does not go far enough.

The conclusion derived for RhC that non-relativistic predictions are overestimating the Δg shift seems to be not valid for most of the transition metal doublets of our test set. In this context it is interesting to mention the case of PdH which has also been investigated in the work of Neyman[80] using a

relativistic density functional Douglas–Kroll method. Despite the relativistic approach the obtained Δg shift of 247 ppt is not better than the non-relativistic SOMF prediction.

For completeness we also investigated the performance of relativistic approaches in predicting the g-tensor shifts in this extended set of radical doublets. We consider both the perturbative treatment (ORCA) and the two-component methods (ADF). The spin–orbit interaction is limited to the effective potential approach in order to compare the results on equal footing. In this approach the SOO is omitted and no scale factor is introduced to correct for the unrealistic exchange part.

Fig. 4 displays the differences in $\Delta g_{\mathrm{ortho}}$ reported by the various relativistic approaches for all diatomic doublet molecules tabulated in Table 6, extended with some heavier elements. The ZORA routine in ADF makes use of the relativistic two-component method of van Lenthe for the evaluation of the spin–orbit matrix elements. A TZP basis set is used. Similar relativistic model is built in BAND. In ORCA the V_{eff} method with ZORA Hamiltonian is considered together with a triple-ζ basis set with 2df polarization functions.

For the light elements, Fig. 4 reveals that the predictions of the different programs are very close to each other, which is not surprising since they only differ in whether the spin–orbit elements were calculated perturbatively or not. For light elements the spin–orbit interaction is indeed supposed to be small. For the heavier elements, however, the deviations become more and more significant, possibly indicating a failure of the perturbative approach.

But despite the same relativistic model the largest deviations from ZORA-ADF are observed for BAND. It was already noted that the g-tensor shows a fluctuating rather than a convergence pattern, caused by interactions between periodic images (see Fig. 3).

A correlation diagram with the experimental data is given in the ESI.†

Conclusion: The set of radical doublets confirms what has been concluded from the particular assessment of RhC: the full treatment in SOMF is always preferable but the proposed modification of the effective potential method makes

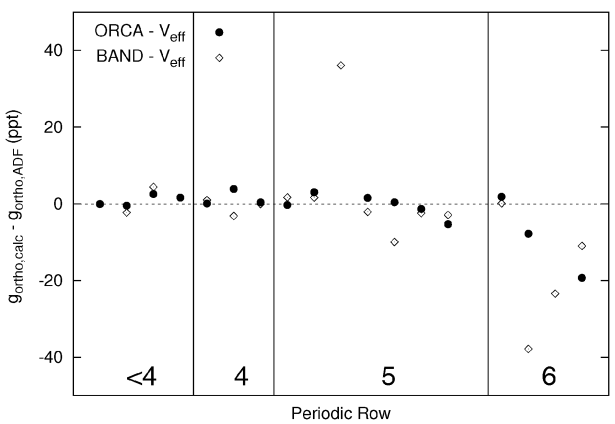

Fig. 4 $\Delta g_{\mathrm{ortho,calc}} - \Delta g_{\mathrm{ortho,ADF}}$ (in ppt) for several doublet molecules, ordered by it's weight. Results of ORCA (with ZORA and V_{eff}) and BAND are compared to the two-component method of ADF. For all calculations a triple-ζ quality basis set with polarization functions (Ahlrichs 2df if possible) was used.

$V_{\mathrm{eff,SOO}}(\sigma = -2)$ an even accurate procedure for predicting g-tensors in transition metal containing doublets due to the robustness of the scale factor σ. A new feature is that this scaling protocol applicable to exchange contributions is also transferable to periodic codes, but with a slightly larger scale factor. We suggest to use $\sigma = -2.8$.

4.3 High spin radicals

For the high spin radicals we select a training set as used by Patchkovskii *et al.*[33] Features observed in the radical doublets will be tested on its transferability to high spin systems with spins varying from 1 to 3.

The results are tabulated in Table 8. The experimental agreement is very good and the largest deviation from experiment is even substantially smaller (less than 50 ppm) than in the training set of radical doublets.

It is clear that the results concerning the exchange contribution formulated for spin-$\frac{1}{2}$ molecules still hold.

The SOMF SO(2e) exchange values are all small but they have to be multiplied with a factor of three to account for the spin–other-orbit corrections before they can be added to the direct Coulomb contribution. The remarkable feature of a quasi constant scale factor relating the exchange contributions between the mean field and the effective potential model still holds. The robustness of the scale factor σ' throughout the whole set of high spin molecules is even better than for the radical doublets. These features have not been assessed and reported before, and therefore very useful to communicate in the recommendation of suitable protocols for g-tensor computations of non-isolated molecules, where periodic codes are obviously more recommended than gas-phase computations.

In Table 8 the direct Coulomb two-electron contribution ($\mathrm{SO(2e)_{direct}}$) does not involve the additional terms arising from the spin–other-orbit (SOO) interaction. In ref. 71 they have been omitted. In the theoretical section we demonstrated the existence of these extra terms, which are only increasing in importance the higher the spin.

In Table 9 results of calculations including and excluding this direct SOO contribution are reported and compared to experimental values. It is clear that this is a non-negligible contribution, which can contribute more than 20% of the total Δg. For molecules with small Δg values, it can even be the dominant contribution. In several cases, the accuracy can be improved quite substantially.

There are, however, some particular cases where the discrepancy with experiment remains large, despite the additional correction terms arising from the direct contribution to the SOO coupling. The origin of these large deviations should be found elsewhere. Changing the internuclear distances does not really improve the experimental agreement. Incorrect KS orbitals could lie at the origin, but this investigation falls outside the scope of this paper. The assumption of isolated molecules in the theoretical calculations might not strike reality when compared to the experimental setup.

5 Conclusion

In this paper an overview is given of all key factors playing a role in the accurate reproduction of the g-tensor of a transition

Table 8 Various spin–orbit contributions to the Δg_{ortho} shift in ppt for several high-spin molecules. Molecules are ranked per spin multiplicity according to the heaviest element. All calculations were performed with PBE and a Ahlrichs TZV 2df. The scaling factors σ and σ' are defined in eqn (19) and (20) respectively

			ORCA					CP2K			
					SO(2e)	SO(2e) exch					
		Spin	ZKE	SO(N)	Direct	SOMF	∇v_{xc}	SO(N) + $SO(2e)_{dir}$	SO(2e) ∇v_{xc}	Scale factor σ	Scale factor σ'
<4	B_2	1	−0.08	0.48	−0.18	−0.03	0.05	0.26	0.03	−1.73	−2.45
<4	*NH*	1	−0.20	2.11	−0.55	−0.09	0.14	1.56	0.11	−1.89	−2.41
<4	*NF*	1	−0.27	2.82	−0.53	−0.10	0.15	2.22	0.12	−2.11	−2.67
<4	*NCl*	1	−0.24	6.84	−0.93	−0.17	0.24	5.84	0.19	−2.08	−2.69
4	*NBr*	1	−0.23	21.59	−1.55	−0.25	0.37	19.91	0.28	−2.06	−2.69
5	*NI*	1	−0.21	−0.47	0.14	0.02	−0.03	−0.22	−0.03	−2.15	−2.41
<4	O_2	1	−0.35	3.98	−0.81	−0.17	0.23	3.11	0.18	−2.23	−2.84
<4	*PH*	1	−0.15	−1.80	6.43	−0.11	0.16	4.60	0.13	−2.03	−2.56
4	*SeO*	1	−0.27	18.32	−1.48	−0.28	0.39	16.48	0.30	−2.15	−2.79
<4	*SO*	1	−0.27	6.58	−1.01	−0.21	0.28	5.45	0.22	−2.24	−2.87
<4	S_2	1	−0.23	16.68	−2.03	−0.32	0.45	14.59	0.35	−2.15	−2.79
<4	*BC*	3/2	−0.11	0.12	−0.04	0.01	0.00	0.07	0.01	7.52	2.67
<4	C_2^+	3/2	−0.15	−0.57	0.15	0.05	−0.05	−0.44	−0.02	−3.24	−6.43
<4	*AlC*	3/2	−0.12	−1.84	0.35	0.06	−0.08	−1.59	−0.05	−2.33	−3.67
<4	*SiB*	3/2	−0.10	−1.42	0.30	0.06	−0.08	−1.19	−0.05	−2.29	−3.60
<4	*SiAl*	3/2	−0.10	−5.14	0.81	0.13	−0.18	−4.40	−0.12	−2.14	−3.02
<4	Si_2^+	3/2	−0.12	−7.98	1.19	0.19	−0.26	−6.74	−0.18	−2.15	−3.04
4	*VO*	3/2	−0.36	−29.98	12.60	1.00	−1.28	−18.02	−0.95	−2.36	−3.15
4	*TiV*	3/2	−0.39	−26.94	11.97	0.90	−1.15	−16.37	−0.89	−2.34	−3.02
4	V_2^+	3/2	−0.35	−18.95	8.12	0.61	−0.78	−12.06	−0.61	−2.34	−2.98
4	*CrN*	3/2	−0.49	−7.18	2.79	0.25	−0.30	−4.54	−0.21	−2.44	−3.53
4	Ge_2^+	3/2	−0.14	−49.65	3.84	0.46	−0.67	−45.63	−0.49	−2.08	−2.83
4	$GaAs^+$	3/2	−0.17	−19.73	1.64	0.19	−0.27	−17.85	−0.19	−2.06	−2.93
5	YB^+	3/2	−0.14	−57.86	17.12	1.01	−1.39	−41.15	−1.01	−2.18	−2.98
5	YAl^+	3/2	−0.15	−100.80	28.53	1.66	−2.30	−73.10	−1.70	−2.17	−2.94
5	*ZrV*	3/2	−0.40	−40.90	15.80	1.11	−1.45	−26.47	−1.09	−2.30	−3.06
5	*MoN*	3/2	−0.36	−6.44	1.46	0.11	−0.14	−5.66	−0.10	−2.37	−3.37
5	*NbO*	3/2	−0.28	−47.61	12.77	0.78	−1.05	−36.05	−0.79	−2.23	−2.97
5	*TiNb*	3/2	−0.34	−43.71	14.50	0.94	−1.25	−31.18	−0.95	−2.27	−2.99
5	*ZrNb*	3/2	−0.32	−63.89	18.16	1.05	−1.43	−47.20	−1.06	−2.21	−2.97
4	*CrF*	5/2	−0.48	−16.49	6.32	0.46	−0.58	−10.66	−0.43	−2.36	−3.20
5	*CrAg*	5/2	−0.51	−0.34	0.58	0.05	−0.07	0.07	−0.04	−2.42	−3.79
4	*MnO*	5/2	−0.57	5.52	−2.35	−0.19	0.27	2.82	0.21	−2.14	−2.83
4	*MnS*	5/2	−0.59	16.89	−5.81	−0.43	0.59	10.40	0.44	−2.18	−2.92
4	*MnH*	3	−0.57	0.08	−0.93	−0.05	0.06	−0.93	0.06	−2.35	−2.52
4	*MnF*	3	−0.58	1.85	−0.94	−0.07	0.10	0.99	0.09	−3.30	−3.54
4	*MnCl*	3	−0.57	3.13	−1.26	−0.09	0.13	2.06	0.11	−2.19	−2.41
4	*MnBr*	3	−0.57	7.93	−1.65	−0.13	0.18	6.69	0.16	−2.15	−2.46
5	*MnAg*	3	−0.58	5.69	−2.19	−0.12	0.17	3.87	0.15	−2.22	−2.50

metal containing system using DFT-based methods: choice of a relativistic Hamiltonian, spin–orbit approximation, gauge corrections of the magnetic vector potential, *etc*. Special attention has been given to the description of the spin–orbit interaction and the contributions of the spin–other-orbit coupling term to the *g*-tensor. A new protocol has been suggested to improve the performance of periodic codes to predict *g*-tensors.

The conclusions of this work can be summarized in two parts:

(i) an effective method has been proposed to correct the unrealistic character of the exchange contribution in periodic codes like CP2K, bringing their *g*-tensor predictions at the same accuracy as those obtained in computationally more expensive spin–orbit mean-field models. A remarkable relationship has been noticed between the two-electron spin–orbit matrix elements and the unrealistic $\Delta g(\nabla v_{xc})$ predictions in the effective potential model within the KS scheme. An almost constant scale factor is found throughout the whole set of radical doublets and high-spin systems relating the wrong V_{eff} exchange contribution to the correct SOMF prediction. In this work a scale factor of about −2.80 is proposed, which is somewhat larger than the factor of −2 proposed by Neese, but bringing the DFT predictions in periodic codes close to those resulting from the computationally more expensive SOMF-ORCA calculations. It opens new perspectives for using periodic codes in the calculation of *g*-tensors in large extended systems containing transition metals.

(ii) for high spin states there appear some extra contributions to the direct Coulomb term belonging to the spin–other-orbit term. This is a direct consequence of the fact that in these systems multiple single occupied molecular orbitals are present. We found that these additional contributions are not negligible and improve the experimental agreement in most of the cases.

Concluding, with the implementation of the scale factor for the exchange contribution and the extra SOO terms for high-spin systems, CP2K has become a viable code for calculating *g*-tensors in periodic systems containing transition elements.

Table 9 The inclusion of the direct contribution of the SOO coupling is compared to previous results. All calculations were performed in CP2K using a TZV 2df basis set and PBE functional. A scaling factor of $\sigma' = -2.8$ is used

	CP2K							CP2K	
	Spin	Exp	$V_{\text{eff,SOO}}$	$V^{*}_{\text{eff,SOO}}$		Spin	Exp	$V_{\text{eff,SOO}}$	$V^{*}_{\text{eff,SOO}}$
B_2	1	−0.8	0.09	0.21	CrN	3/2	−5.6	−4.41	−5.02
NH	1	1.7	1.02	1.24	Ge_2^+	3/2	−63.3	−44.29	−44.66
NF	1	2.0	1.60	1.78	$GaAs^+$	3/2	−4.5	−17.44	−17.55
NCl	1	5.4	5.03	5.28	YB^+	3/2	−42.3	−38.25	−40.20
NBr	1	19.3	18.83	19.18	YAl^+	3/2	−60.3	−68.16	−71.33
NI	1	31.0	−0.34	−0.36	ZrV	3/2	−41.3	−23.60	−27.56
O_2	1	2.9	2.22	2.40	MoN	3/2	−10.9	−5.72	−5.70
PH	1	4.5	4.07	4.24	NbO	3/2	−44.6	−33.97	−35.23
SeO	1	32.7	15.30	15.63	$TiNb$	3/2	−73.8	−28.68	−31.46
SO	1	3.6	4.53	4.74	$ZrNb$	3/2	−98.8	−44.34	−46.22
$S2$	1	14.5	13.31	13.64	CrF	5/2	−1.3	−9.86	−11.56
BC	3/2	−0.3	−0.08	−0.02	$CrAg$	5/2	1.7	−0.32	−0.49
C_2^+	3/2	−0.5	−0.51	−0.48	MnO	5/2	−7.3	1.62	2.36
AlC	3/2	−1.3	−1.50	−1.53	MnS	5/2	6.7	8.47	9.94
SiB	3/2	−1.8	−1.14	−1.17	MnH	3	−1.3	−1.661	−1.35
$SiAl$	3/2	−4.5	−4.13	−4.23	MnF	3	−1.3	0.13	0.47
Si_2^+	3/2	−9.3	−6.31	−6.49	$MnCl$	3	−7.3	1.14	1.54
VO	3/2	−21.9	−15.52	−19.25	$MnBr$	3	−9.3	5.65	6.14
TiV	3/2	−24.3	−14.08	−17.96	$MnAg$	3	−4.3	2.84	3.33
V_2^+	3/2	−46.3	−10.56	−13.20					

6 Appendix: spin–orbit mean field

In this appendix we reformulate the Spin–Orbit Mean-Field (SOMF) method and focus on the contribution of the direct part of the two-body spin–other-orbit contribution which is non-negligible for high-spin complexes.

Two-body interactions can be best treated within second quantization formalism:

$$\frac{1}{2}\sum_{ij}\hat{V}_{ij} \rightarrow \frac{1}{4}\sum_{\alpha\beta\gamma\delta}\langle\alpha\beta|V_{12}|\gamma\delta\rangle_{\text{as}}c_{\alpha}^{\dagger}c_{\beta}^{\dagger}c_{\delta}c_{\gamma} \tag{21}$$

with the antisymmetric matrix element $\langle\alpha\beta|V_{12}|\gamma\delta\rangle_{\text{as}} = \langle\alpha\beta|V_{12}|\gamma\delta\rangle - \langle\alpha\beta|V_{12}|\delta\gamma\rangle$ and α, β, γ and δ as single-electron spin orbitals, represented by creation ($c_{\alpha}^{\dagger}$, $c_{\beta}^{\dagger}$) and annihilation operators (c_{δ}, c_{γ}). The two-body interaction should be first made symmetric with interchange of i and j. The two-body matrix element of the two-electron spin–orbit interaction can then be written as a product in spin and real space:

$$\begin{aligned}\langle\alpha\beta|V_{12}^{\text{SO(2e)}}|\gamma\delta\rangle_{\text{as}} = &-\tfrac{1}{2}\,\delta_{m_{s,b}\,m_{s,d}}\,\langle m_{s,a}|\boldsymbol{s}|m_{s,c}\rangle\cdot\langle ab|\boldsymbol{L}_1|cd\rangle\\ &-\tfrac{1}{2}\,\delta_{m_{s,a}\,m_{s,c}}\,\langle m_{s,b}|\boldsymbol{s}|m_{s,d}\rangle\cdot\langle ab|\boldsymbol{L}_1|dc\rangle\end{aligned} \tag{22}$$

with $\boldsymbol{L}_1 = \frac{\alpha^2}{r_{12}^3}(\boldsymbol{r}_{12}\times\boldsymbol{p}_1)$ which coincides with $-2g^{\text{soc}}(1,2)$ introduced by Neese.[71] In eqn (22) the spin–orbital α is decomposed in the spatial orbital a and spin $m_{s,a}$.

Similar to the spin–other-orbit interaction one gets

$$\begin{aligned}\langle\alpha\beta|V_{12}^{\text{SOO}}|\gamma\delta\rangle_{\text{as}} = &-\tfrac{1}{2}\,\delta_{m_{s,b}\,m_{s,d}}\,\langle m_{s,a}|\boldsymbol{s}|m_{s,c}\rangle\cdot\langle ba|\boldsymbol{L}_1|dc\rangle\\ &-\tfrac{1}{2}\,\delta_{m_{s,a}\,m_{s,c}}\,\langle m_{s,b}|\boldsymbol{s}|m_{s,d}\rangle\cdot\langle ab|\mathbf{L}_1|cd\rangle\end{aligned} \tag{23}$$

One easily observes that the two spin–orbit interactions turn out to show a linear relationship only when the spins of all spin orbitals are equal to each other.

In the first order perturbation the most elementary excitation of the ground-state Slater determinant $|\Psi^{(0)}\rangle$ as SCF response to some external perturbation V^{λ} is the substitution of one of the unperturbed occupied orbitals h by its perturbed orbital $h^{(1)}$

$$|h^{(1)}\rangle = \sum_{p\in\text{virt}}\frac{V_{ph}^{\lambda}}{\varepsilon_p - \varepsilon_h}|p\rangle \tag{24}$$

with a sum over all zeroth order virtual orbitals p.

For the further evaluation of the matrix elements it is sufficient to consider a single one-electron particle–one electron hole excitation ($|\Psi^{1}\rangle = c_p^{\dagger}c_h|\Psi^{(0)}\rangle$) where an occupied orbital h is replaced by a virtual orbital p; also called singly substituted determinants.

In the second quantization one gets the standard expression valid for any two-body interaction

$$\begin{aligned}&\left\langle\Psi^{(0)}\middle|\frac{1}{2}\sum_{ij}V_{ij}\middle|\Psi^{(1)}\right\rangle\\ &\quad=\frac{1}{4}\sum_{\alpha\beta\gamma\delta}\langle\alpha\beta|V_{12}|\gamma\delta\rangle_{\text{as}}\langle\Psi^{(0)}|c_{\alpha}^{\dagger}c_{\beta}^{\dagger}c_{\delta}c_{\gamma}c_{p}^{\dagger}c_{h}|\Psi^{(1)}\rangle\end{aligned} \tag{25}$$

$$=\sum_{\alpha\in\text{occ}}\langle h\alpha|V_{12}|p\alpha\rangle_{\text{as}} = \langle h|\Gamma^{\text{SO}}|p\rangle \tag{26}$$

determining the spin–orbit mean-field Γ^{SO}, completely similar as in mean-field approaches appropriate in interacting many-particle problems. For paramagnetic centers with only one singly occupied spin orbital h, the summation runs over all paired occupied molecular orbitals, hence $\sum_{\alpha\in\text{OCC}} = \sum_{a\in\text{OCC}}\sum_{m_{s,a}}$.

For the two-electron spin–orbit interaction the contribution to the spin–orbit mean-field becomes

$$\begin{aligned}&\sum_{\alpha\in\text{occ}}\langle h\alpha|V_{12}^{\text{SO(2e)}}|p\alpha\rangle_{\text{as}}\\ &=-\frac{1}{2}\sum_{a\in\text{occ}}\langle ha|L_{1z}|pa\rangle+\frac{1}{4}\sum_{a\in\text{occ}}\left(\langle ha|L_{1z}|ap\rangle+\langle ah|L_{1z}|pa\rangle\right)\end{aligned} \tag{27}$$

The above expression only holds if the spin of the molecular orbital h is equal to that of the scattered state p: $m_{s,h} = m_{s,p} = \frac{1}{2}$. The first term is the direct Coulomb integral, while the second is the exchange contribution. For the spin–other-orbit interaction, one gets somewhat similar expression:

$$\sum_{a\in\mathrm{occ}} \langle h\alpha|V_{12}^{\mathrm{SOO}}|p\alpha\rangle_{\mathrm{as}} = -\sum_{a\in\mathrm{occ}} \langle ah|L_{1z}|ap\rangle + \frac{1}{2}(\langle ah|L_{1z}|pa\rangle + \langle ha|L_{1z}|ap\rangle) \quad (28)$$

but with the fundamental difference that now the direct Coulomb term is disappearing.

For real spatial wave functions the single-particle matrix elements for the Hermitian momentum operator becomes $\langle a|\boldsymbol{p}|a\rangle = \langle a|p|a\rangle^* = \langle a|\boldsymbol{p}^*|a\rangle = -\langle a|\boldsymbol{p}|a\rangle = 0$, and hence also the two-body matrix element of the spin–orbit operator $\boldsymbol{L}_1$ will disappear ($\langle ah|\boldsymbol{L}_1|ap\rangle = 0$). Concluding, for spin-$\frac{1}{2}$ complexes the spin–other-orbit interactions only contribute by means of their exchange term. In addition, inspection of eqn (27) and (28) immediately learns that the exchange SOO contribution is exactly twice the exchange contribution of the SO(2e) term:

$$\sum_{\alpha\in\mathrm{occ}} \langle h\alpha|V_{12}^{\mathrm{SOO}}|\alpha p\rangle = 2\sum_{\alpha\in\mathrm{occ}} \langle h\alpha|V_{12}^{\mathrm{SO(2e)}}|\alpha p\rangle \quad (29)$$

This relation is also valid for high spin complexes.

Finally, the spin–orbit mean field I^{SO} is then obtained as

$$\langle h|I^{\mathrm{SO}}|p\rangle = -\frac{1}{2}\sum_{a\in\mathrm{occ}} \langle ha|L_{1z}|pa\rangle + \frac{3}{4}\sum_{a\in\mathrm{occ}} (\langle ha|L_{1z}|ap\rangle + \langle ah|L_{1z}|pa\rangle) \quad (30)$$

The derivation of the expressions, presented in this work, differs slightly from those of Neese[71] and others.[75] However, the final results are equivalent.

Application of eqn (30) to evaluate the Δg^{SO} correction is the so-called spin–orbit mean-field (SOMF) approach, as implemented in ORCA. It is an excellent starting platform to estimate the contribution of the spin–other-orbit (SOO) correction for spin-$\frac{1}{2}$ molecules.

The extension to higher spin states can easily be performed. Instead of one we now consider 2 S singly occupied molecular orbitals β where S represents the total spin of the molecular system. The contribution to the spin–orbit mean-field from the two-electron spin–orbit interaction becomes

$$\sum_{\gamma=\alpha,\beta\mathrm{occ}} \langle h\gamma|V_{12}^{\mathrm{SO(2e)}}|p\gamma\rangle = -\frac{1}{2}\sum_{a\in\mathrm{occ}} \langle ha|L_{1z}|pa\rangle - \frac{1}{4}\sum_{b\in\mathrm{occ}} \langle hb|L_{1z}|pb\rangle + \frac{1}{4}\sum_{c=a,b\in\mathrm{occ}} (\langle hc|L_{1z}|cp\rangle + \langle ch|L_{1z}|pc\rangle) \quad (31)$$

Only in the direct Coulomb term one notices some slight difference in comparison with the spin 1/2 systems. As the b-orbitals are singly occupied they only half contribute to the mean field.

In contrast to the spin 1/2 systems, there is now a non-vanishing contribution from the spin–other-orbit interaction in higher spin molecules to the direct Coulomb term:

$$-\frac{1}{2}\sum_{b=\mathrm{hocc}} \langle hb|L_{1z}|pb\rangle \quad (32)$$

This is not really negligible for high spin systems, *e.g.* diatomic molecules with Mn as element whose ground state configuration generates spin 3 with 6 singly occupied molecular orbitals with parallel spin. In this case of high spin our results apparently differ from those of Neese. On the other hand, the exchange contribution $\mathrm{SOO}_{\mathrm{exch}}$ still obeys relation (8).

Acknowledgements

The authors would like to thank the Fund for Scientific Research (FWO-Flanders, Belgium) and the Research Board of Ghent University for financial support. Part of the computational resources and services used in this work were provided by Ghent University.

References

1 M. Kaupp, M. Bühl and V. G. Malkin, *Calculation of NMR and EPR Parameters*, WILEY-VCH4, 2004.
2 D. A. Case, *J. Chem. Phys.*, 1985, **83**, 5792–5796.
3 E. van Lenthe, P. E. S. Wormer and A. van der Avoird, *J. Chem. Phys.*, 1997, **107**, 2488.
4 K. M. Neyman, D. I. Ganyushin, A. V. Matveev and V. A. Nasluzov, *J. Phys. Chem. A*, 2002, **106**, 5022–5030.
5 O. Vahtras, M. Engström and B. Schimmelpfennig, *Chem. Phys. Lett.*, 2002, **434**, 424–430.
6 R. Declerck, V. Van Speybroeck and M. Waroquier, *Phys. Rev. B: Condens. Matter Mater. Phys.*, 2006, **73**, 115113.
7 F. Neese, *J. Chem. Phys.*, 2001, **115**, 11080–11096.
8 C. J. Pickard and F. Mauri, *Phys. Rev. Lett.*, 2002, **88**, 086403.
9 V. Weber, M. Iannuzzi, S. Giani, J. Hutter, R. Declerck and M. Waroquier, *J. Chem. Phys.*, 2009, **131**, 014106.
10 E. S. Kadantsev and T. Ziegler, *J. Phys. Chem. A*, 2009, **113**, 1327.
11 E. Pauwels, R. Declerck, V. Van Speybroeck and M. Waroquier, *Radiat. Res.*, 2008, **169**, 8.
12 E. Pauwels, R. Declerck, T. Verstraelen, B. De Sterck, C. W. M. Kay, V. Van Speybroeck and M. Waroquier, *J. Phys. Chem. B*, 2010, **113**, 16655.
13 E. Pauwels, H. De Cooman, M. Waroquier, E. O. Hole and E. Sagstuen, *Phys. Chem. Chem. Phys.*, 2010, **12**, 8733.
14 F. Pietrucci, M. Bernasconi, C. Di Valentin, F. Mauri and C. J. Pickard, *Phys. Rev. B: Condens. Matter Mater. Phys.*, 2006, **73**, 134112.
15 N. Sakhabutdinova, A. Van Yperen-De Deyne, V. Van Speybroeck, E. Pauwels, H. Vrielinck, F. Callens and M. Waroquier, *J. Phys. Chem. A*, 2011, **115**, 1721–1733.
16 W. M. Ames and S. C. Larsen, *J. Phys. Chem. A*, 2010, **114**, 589.
17 K. Pierloot, A. Delabie, M. H. Groothaert and R. A. Schoonheydt, *Phys. Chem. Chem. Phys.*, 2001, **3**, 2174–2183.
18 M. Danilczuk and A. Lund, *Chem. Phys. Lett.*, 2010, **490**, 205–209.
19 G. te Velde, F. M. Bickelhaupt, E. J. Baerends, C. F. Guerra, S. J. A. Van Gisbergen, J. G. Snijders and T. Ziegler, *J. Comput. Chem.*, 2001, **22**, 931–967.
20 C. F. Guerra, J. G. Snijders, G. te Velde and E. J. Baerends, *Theor. Chem. Acc.*, 1998, **99**, 391–403.
21 E. Baerends, T. Ziegler, J. Autschbach, D. Bashford, A. Brces, F. Bickelhaupt, C. Bo, P. Boerrigter, L. Cavallo, D. Chong, L. Deng, R. Dickson, D. Ellis, M. van Faassen, L. Fan, T. Fischer, C. F. Guerra, A. Ghysels, A. Giammona, S. van Gisbergen, A. Gtz, J. Groeneveld, O. Gritsenko, M. Grning, S. Gusarov, F. Harris, P. van den Hoek, C. Jacob, H. Jacobsen, L. Jensen, J. Kaminski, G. van Kessel, F. Kootstra, A. Kovalenko, M. Krykunov, E. van Lenthe, D. McCormack, A. Michalak,

M. Mitoraj, J. Neugebauer, V. Nicu, L. Noodleman, V. Osinga, S. Patchkovskii, P. Philipsen, D. Post, C. Pye, W. Ravenek, J. RodrÃguez, P. Ros, P. Schipper, G. Schreckenbach, J. Seldenthuis, M. Seth, J. Snijders, M. Sol, M. Swart, D. Swerhone, G. te Velde, P. Vernooijs, L. Versluis, L. Visscher, O. Visser, F. Wang, T. Wesolowski, E. van Wezenbeek, G. Wiesenekker, S. Wolff, T. Woo and A. Yakovlev, *ADF2009.01, SCM*, http://www.scm.com.
22 http://www.thch.uni-bonn.de/tc/orca/.
23 M. J. Frisch, G. W. Trucks, H. B. Schlegel, G. E. Scuseria, M. A. Robb, J. R. Cheeseman, G. Scalmani, V. Barone, B. Mennucci, G. A. Petersson, H. Nakatsuji, M. Caricato, X. Li, H. P. Hratchian, A. F. Izmaylov, J. Bloino, G. Zheng, J. L. Sonnenberg, M. Hada, M. Ehara, K. Toyota, R. Fukuda, J. Hasegawa, M. Ishida, T. Nakajima, Y. Honda, O. Kitao, H. Nakai, T. Vreven, J. A. Montgomery Jr, J. E. Peralta, F. Ogliaro, M. Bearpark, J. J. Heyd, E. Brothers, K. N. Kudin, V. N. Staroverov, R. Kobayashi, J. Normand, K. Raghavachari, A. Rendell, J. C. Burant, S. S. Iyengar, J. Tomasi, M. Cossi, N. Rega, J. M. Millam, M. Klene, J. E. Knox, J. B. Cross, V. Bakken, C. Adamo, J. Jaramillo, R. Gomperts, R. E. Stratmann, O. Yazyev, A. J. Austin, R. Cammi, C. Pomelli, J. W. Ochterski, R. L. Martin, K. Morokuma, V. G. Zakrzewski, G. A. Voth, P. Salvador, J. J. Dannenberg, S. Dapprich, A. D. Daniels, Farkas, J. B. Foresman, J. V. Ortiz, J. Cioslowski and D. J. Fox, *Gaussian 09 Revision A.1*, Gaussian Inc, Wallingford, CT, 2009.
24 *DALTON, a molecular electronic structure program, Release 2.0*, 2005, http://daltonprogram.org/.
25 O. L. Malkina, J. Vaara, B. Schimmelpfennig, M. Munzarová, V. G. Malkin and M. Kaupp, *J. Am. Chem. Soc*., 2000, **122**, 9206.
26 C. J. Pickard and F. Mauri, *Phys. Rev. B: Condens. Matter Mater. Phys*., 2001, **63**, 245101.
27 P. Giannozzi, S. Baroni, N. Bonini, M. Calandra, R. Car, C. Cavazzoni, D. Ceresoli, G. L. Chiarotti, M. Cococcioni, I. Dabo, A. Dal Corso, S. de Gironcoli, S. Fabris, G. Fratesi, R. Gebauer, U. Gerstmann, C. Gougoussis, A. Kokalj, M. Lazzeri, L. Martin-Samos, N. Marzari, F. Mauri, R. Mazzarello, S. Paolini, A. Pasquarello, L. Paulatto, C. Sbraccia, S. Scandolo, G. Sclauzero, A. P. Seitsonen, A. Smogunov, P. Umari and R. M. Wentzcovitch, *J. Phys.: Condens. Matter*, 2009, **21**, 395502(19pp).
28 G. Lippert, J. Hutter and M. Parrinello, *Theor. Chem. Acc*., 1999, **103**, 124–140.
29 T. Laino, F. Mohamed, A. Laio and M. Parrinello, *J. Chem. Theor. Comput*., 2005, **1**, 1176–1184.
30 J. VandeVondele, M. Krack, F. Mohamed, M. Parrinello, T. Chassaing and J. Hutter, *Comput. Phys. Commun*., 2005, **167**, 103–128.
31 P. H. T. Philipsen, G. te Velde, E. J. Baerends, J. A. Berger, P. L. de Boeij, J. A. Groeneveld, E. S. Kadentsev, R. Klooster, K. F. P. Romaniello, D. G. Skachkov, J. G. Snijders, G. Wiesenekker and T. Ziegler, *BAND2010*, http://www.scm.com.
32 A. V. Arbuznikov, M. Kaupp, V. G. Malkin, R. Reviakine and O. L. Malkina, *Phys. Chem. Chem. Phys*., 2002, **4**, 5467.
33 S. Patchkovskii and T. Ziegler, *J. Phys. Chem. A*, 2001, **105**, 5490.
34 I. Malkin, O. L. Malkina, V. G. Malkin and M. Kaupp, *J. Chem. Phys*., 2005, **123**, 244103.
35 F. Stevens, V. Van Speybroeck, I. Carmichael, F. Callens and M. Waroquier, *Chem. Phys. Lett*., 2006, **421**, 281–286.
36 H. Tan, M. Z. Liao and K. Balasubramanian, *Chem. Phys. Lett*., 1997, **280**, 423–429.
37 J. M. Brom, W. Weltner and W. R. M. Graham, *J. Chem. Phys*., 1972, **57**, 4116–4124.
38 I. Shim and K. A. Gingerich, *Surf. Sci*., 1985, **156**, 623.
39 L. B. Knight, B. W. Gregory, S. T. Cobranchi, D. Feller and E. R. Davidson, *J. Am. Chem. Soc*., 1987, **109**, 3521–3525.
40 M. Tinkham and M. W. P. Strandberg, *Phys. Rev*., 1955, **97**, 951–966.
41 A. E. Douglas and W. E. Jones, *Can. J. Phys*., 1966, **44**, 2241–2258.
42 H. Uehara, *Bull. Chem. Soc. Jpn*., 1969, **42**, 886–889.
43 C. Yamada, Y. Endo and E. Hirota, *J. Chem. Phys*., 1983, **79**, 4159–4166.
44 L. B. Knight, S. T. Cobranchi, J. T. Petty, E. Earl, D. Feller and E. R. Davidson, *J. Chem. Phys*., 1989, **90**, 690.
45 L. B. Knight, S. T. Cobranchi and E. Earl, *J. Chem. Phys*., 1988, **88**, 7348.
46 L. B. Knight, S. T. Cobranchi, J. O. Herlong and C. A. Arrington, *J. Chem. Phys*., 1990, **92**, 5856.
47 L. B. Knight, R. M. Babb, G. M. King, A. J. McKinley, M. D. Morse and C. A. Arrington, *J. Chem. Phys*., 1993, **98**, 4404.
48 L. B. Knight, A. J. McKinley, R. M. Babb, M. D. Morse and C. A. Arrington, *J. Chem. Phys*., 1993, **98**, 6749.
49 Y. M. Hamrick and W. Weltner, *J. Chem. Phys*., 1991, **94**, 3371.
50 M. Cheeseman, R. J. Van Zee, H. L. Flanagan and W. Weltner, *J. Chem. Phys*., 1990, **92**, 1553.
51 J. M. Brom, C. H. Durham and W. Weltner, *J. Chem. Phys*., 1974, **61**, 970–981.
52 L. B. Knight and J. T. Petty, *J. Chem. Phys*., 1988, **88**, 481.
53 L. B. Knight and J. Steadman, *J. Chem. Phys*., 1982, **76**, 3378–3384.
54 K. C. Namiki and T. C. Steimle, *J. Chem. Phys*., 1999, **111**, 6385.
55 R. J. Van Zee, S. Li and W. Weltner, *J. Chem. Phys*., 1995, **103**, 2762.
56 W. Weltner, *Magnetic Atoms and Molecules*, Dover Publications, 1983.
57 A. Carrington, G. N. Currie, D. H. Levy and T. A. Miller, *Mol. Phys*., 1969, **17**, 535–542.
58 L. B. Knight, R. Babb, M. Ray, T. J. Banisaukas, L. Russon, R. S. Dailey and E. R. Davidson, *J. Chem. Phys*., 1996, **105**, 10237.
59 R. J. Van Zee, S. Li and W. J. Weltner, *Chem. Phys. Lett*., 1994, **217**, 381–386.
60 P. Belanzoni, E. van Lenthe and E. J. Baerends, *J. Chem. Phys*., 2001, **114**, 4421.
61 J. P. Perdew, K. Burke and M. Ernzerhof, *Phys. Rev. Lett*., 1996, **77**, 3865–3868.
62 A. Schaefer, H. Horn and R. Ahlrichs, *J. Chem. Phys*., 1992, **97**, 2571.
63 D. A. Pantazis, X. Y. Chen, C. R. Landis and F. Neese, *J. Chem. Theor.Comput*., 2008, **4**, 908–919.
64 The Ahlrichs (2df,2pd,2d2fg,3p2df) polarization functions were obtained from the TurboMole basis set library under ftp.chemie.uni-karlsruhe.de/pub/basen.
65 R. Krishnan, J. S. Binkley, R. Seeger and J. A. Pople, *J. Chem. Phys*., 1980, **72**, 650–654.
66 G. Lippert, J. Hutter and M. Parrinello, *Theor. Chem. Acc*., 1999, **103**, 124–140.
67 N. Troullier and J. L. Martins, *Phys. Rev. B: Condens. Matter Mater. Phys*., 1991, **43**, 1993–2006.
68 P. E. Blochl, *Phys. Rev. B: Condens. Matter Mater. Phys*., 1994, **50**, 17953–17979.
69 G. J. Martyna and M. E. Tuckerman, *J. Chem. Phys*., 1999, **110**, 2810.
70 G. Schreckenbach and T. Ziegler, *J. Phys. Chem. A*, 1997, **101**, 3388–3399.
71 F. Neese, *J. Chem. Phys*., 2005, **122**, 034107.
72 E. van Lenthe, E. J. Baerends and J. G. Snijders, *J. Chem. Phys*., 1993, **99**, 4597–4610.
73 C. van Wullen, *J. Chem. Phys*., 1998, **109**, 392–399.
74 P. Knappe and N. Rösch, *J. Chem. Phys*., 1990, **92**, 1153.
75 B. A. Hess, C. M. Marian, U. Wahlgren and O. Gropen, *Chem. Phys. Lett*., 1996, **251**, 365–371.
76 S. Koseki, M. W. Schmidt and M. S. Gordon, *J. Phys. Chem*., 1992, **96**, 10768–10772.
77 S. Koseki, M. S. Gordon, M. W. Schmidt and N. Matsunaga, *J. Phys. Chem*., 1995, **99**, 12764–12772.
78 S. Koseki, M. W. Schmidt and M. S. Gordon, *J. Phys. Chem. A*, 1998, **102**, 10430–10435.
79 R. Ditchfield, *Mol. Phys*., 1974, **27**, 789–807.
80 K. M. Neyman, D. I. Ganyushin and A. V. Matveev, *J. Phys. Chem. A*, 2002, **106**, 5022–5030.

